

## **SUPPLEMENTAL MATERIAL AND METHODS**

### **Cytokine analysis**

Serum from treated animals was collected and a multiplex assay of the mouse cytokine magnetic 10-Plex Panel (Luminex Life-Technologies©) was performed for quantitative cytokine measurement according to the manufacturer's instructions.

### **Quantification of MCMV**

At the indicated time points of infection, spleen, liver and SG were collected and DNA was extracted using DNeasy Tissue kit following the manufacturer's instructions. Quantification of MCMV titers was performed by qPCR as previously described (1). The data represents IE1 gene copies per organ.

### **Microarray Analysis**

RNA from freshly isolated NK cells or activated adherent NK cells was extracted using RNeasy Mini kit (Qiagen) with on-column DNase step (Qiagen) per the manufacturer's instructions. RNA was then quantified using the DS-11 FX+ Spectrophotometer / Fluorometer (Denovix Inc., Wilmington, DE). RNA (150–300 ng) was used for generating biotinylated cRNA through single-round amplification using the MessageAmpIII RNA Amplification kit following the manufacturer's recommendations (Ambion, ThermoFisher Scientific Inc.). A total of 20 µg of biotinylated cRNA was fragmented and hybridized to Affymetrix murine Mouse Gene 2.0ST (ThermoFisher Scientific Inc.) and scanned at the Protein and Nucleic Acid Facility (Stanford University). Two independent RNA samples were analyzed. The microarray data were analyzed using the Affymetrix Transcriptome Analysis Console. Microarray probe intensity values (CEL files) were background-corrected, summarized and normalized using the Robust Multi-array Average (RMA16) algorithm (2) and subsequently filtered on raw intensity for data in the upper 20-100th percentile using the Expression Suite Software version 1.1 (ThermoFisher Scientific Inc.). We considered genes differentially regulated between freshly isolated NK cells (day 0) and the other conditions that were more than 1.5 fold differentially expressed with a false discovery rate equal to or less than 0.1 and with an ANOVA significance value of equal to or smaller than 0.05. Ingenuity® Pathway Analysis (IPA®) software (Qiagen, Redwood City, CA) was used to predict the biological processes that

the up-regulated genes could be involved in. PCA was performed using ggfortify and ggplot package of Rstudio. The two largest principal components were plotted against one another to assess the relationships between different biological repeats of each sample. A Venn diagram of only up-regulated genes was also displayed using the VennDiagram package in Rstudio. The microarray data has been deposited in the NCBI's Gene Expression Omnibus database (Edgar et al., 2002) and are accessible through GEO Series accession number GSE131522 (<https://www.ncbi.nlm.nih.gov/geo/query/acc.cgi?acc=GSE131522>).

### **In vivo evaluation of NK cell proliferation**

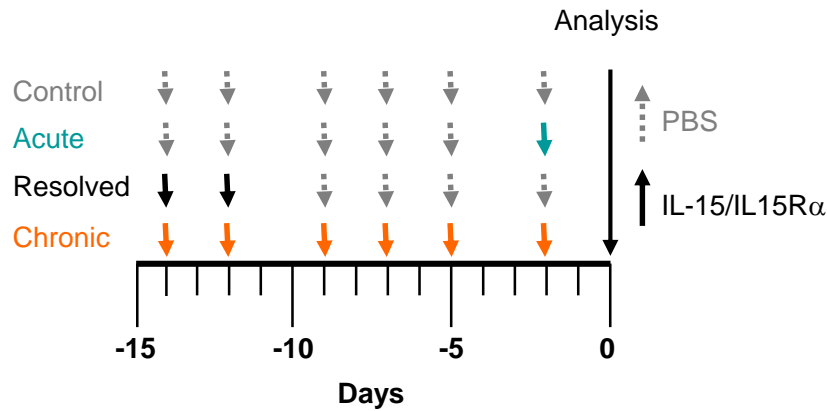
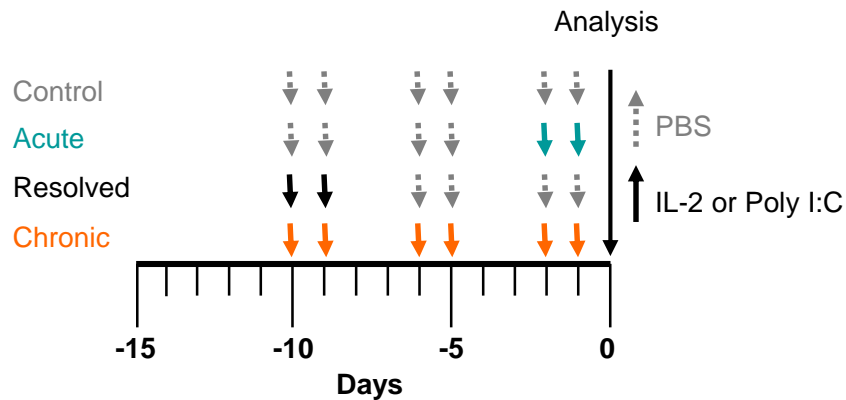
C57BL/6 L2G85 Luc<sup>+</sup> fresh NK cells or ex vivo IL-2 stimulated aNK cells (control aNK or KU treated) were transferred iv. into BALB/c Rag2<sup>-/-</sup>IL2Rc<sup>γ</sup><sup>-/-</sup> deficient mice and treated with 5x10<sup>4</sup> IU IL-2 for 7 days. NK cell proliferation, expansion and survival were measured by bioluminescence at different time points.

### **SUPPLEMENTAL MATERIAL AND METHODS' REFERENCES**

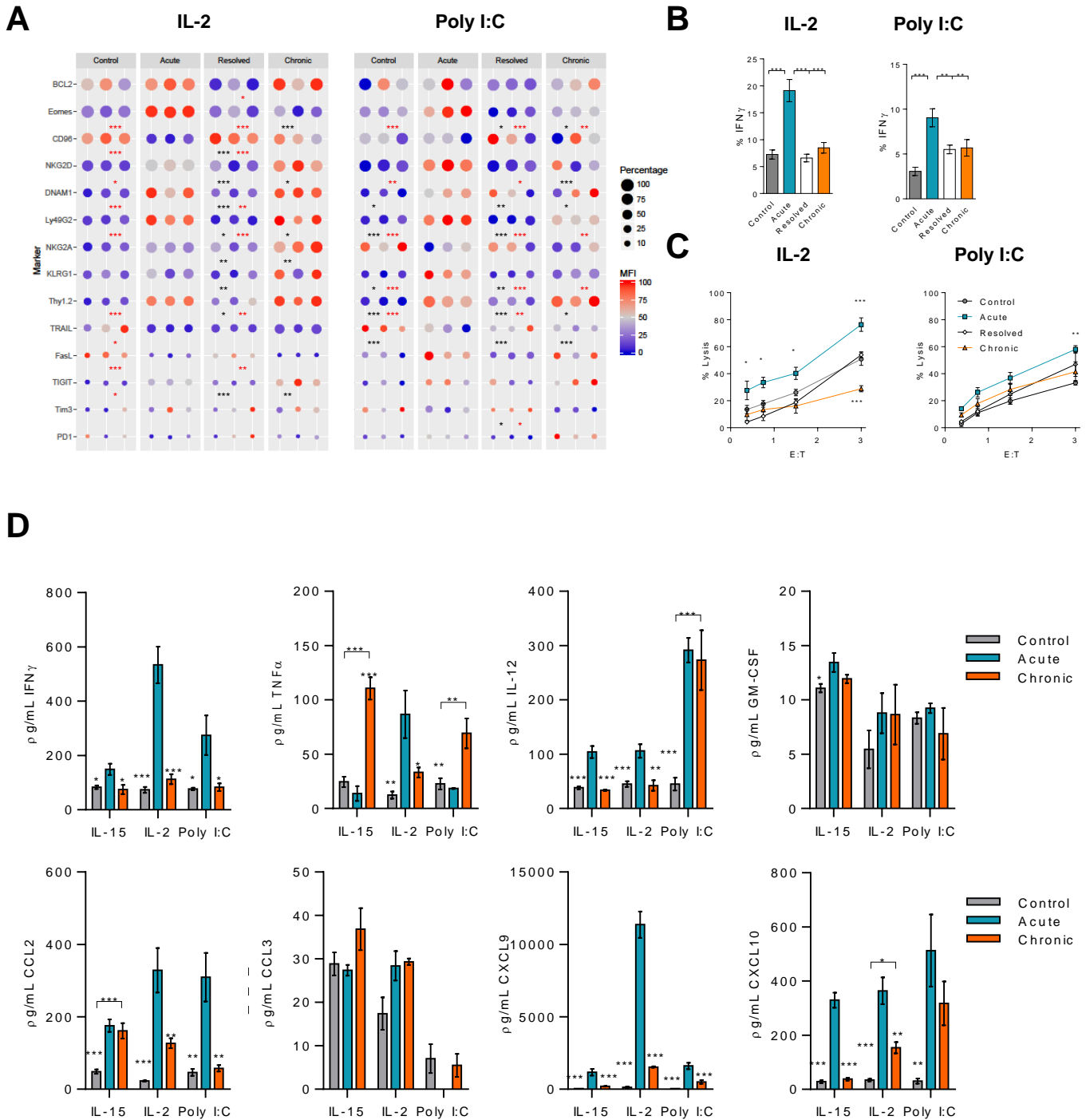
1. M. Alvarez *et al.*, Contrasting effects of anti-Ly49A due to MHC class I cis binding on NK cell-mediated allogeneic bone marrow cell resistance. *Journal of immunology* **191**, 688 (Jul 15, 2013).

Antibody	Clone	Provider	Catalogue
<b>Armenian Hamster IgG</b>		Thermo Fisher Scientific	13-4113-85
<b>Armenian Hamster IgG Isotype Control</b>	eBio299Arm	Thermo Fisher Scientific	14-4888-81
<b>ATM (pSer1981)</b>	10H11.E12	Thermo Fisher Scientific	50-9046-41
<b>BCL2</b>	BCL/10C4	BioLegend	633509
<b>CD122</b>	5H4	BioLegend	105904
<b>CD3</b>	145-2C11	BioLegend	100334, 100355
<b>CD4</b>	RM4-5	BioLegend	100552
<b>CD49b</b>	DX5	BioLegend	108906
<b>CD8</b>	53-6.7	BioLegend	100714, 100744
<b>CD96</b>	3.3	BioLegend	131705
<b>Chk2 (pT68)</b>		Abcam	ab85743
<b>DNAM1</b>	1.00E+06	BioLegend	128803
<b>Eomes</b>	Dan11mag	BioLegend	12-4875-82
<b>FasL</b>	MFL3	Thermo Fisher Scientific	46-5911-82
<b>Granzyme B</b>	GB11	BioLegend	515403
<b>IFN<math>\gamma</math></b>	XMG1.2	BioLegend	505814, 505837
<b>ISo</b>		BioLegend	
<b>Ki67</b>	16A8	BioLegend	652420
<b>KLRG1</b>	2F1/KL1261	BioLegend	138409, 138423
<b>Ly49G2</b>	4D11	BD Bioscience	555315
<b>Ly49H</b>	3D10	Thermo Fisher Scientific	13-5886-81, 50-4875-80
<b>Mouse IgG1, Kappa</b>		Thermo Fisher Scientific	50-4714-80
<b>MULT1</b>	5D10	Thermo Fisher Scientific	12-5863-81, 14-5863-82
<b>NK1.1</b>	PK136	BioLegend	108720, 108722, 108745
<b>NKG2A</b>	16a11	Thermo Fisher Scientific	12-5897-82
<b>NKG2D</b>	CX5	Thermo Fisher Scientific	25-5882-82
<b>PD1</b>	RPM1-30	Thermo Fisher Scientific	17-9981-80
<b>PD1</b>	29F.1A12	BioLegend	135220
<b>Rabbit IgG</b>	Polyclonal	Abcam	Ab171870
<b>Rabbit IgG XP<sup>®</sup></b>	DA1E	Cell signaling Technology	3900S
<b>Rae1d</b>	RD-41	Thermo Fisher Scientific	12-5756-82
<b>Rat IgG1, Kappa</b>	RTK2071	BioLegend	400418, 400443
<b>Streptavidin</b>		Thermo Fisher Scientific, BL	46-4317-82, 405229
<b>TCRb</b>	H57-597	BioLegend	109243, 109226
<b>Thy1.2</b>	30-H12	BioLegend	105324, 105331
<b>TIGIT</b>	1G9	BioLegend	142105
<b>Tim3</b>	RMT3-23	BioLegend	119706, 119715
<b>TRAIL</b>	N2B2	BioLegend	109303
<b>Armenian Hamster IgG</b>		Thermo Fisher Scientific	13-4113-85

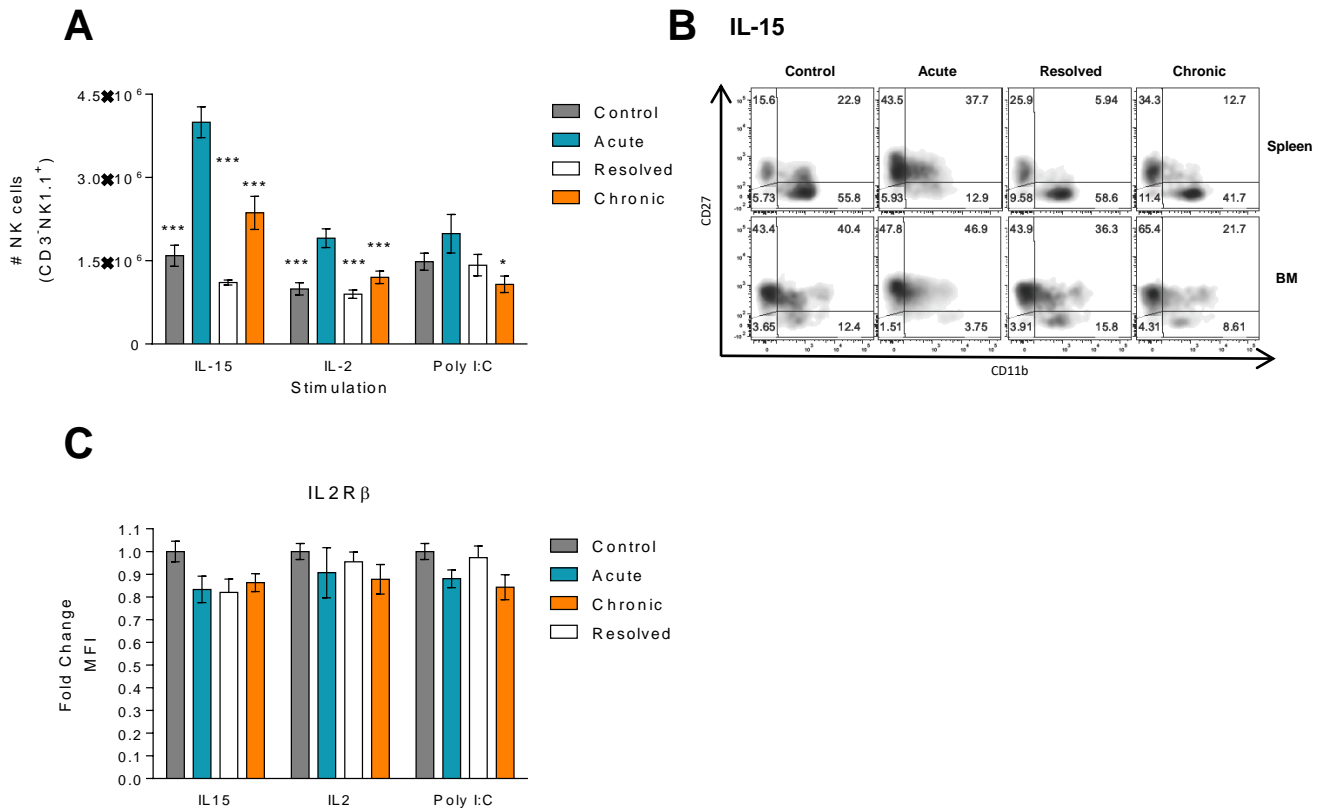
**Supplemental Table 1.** Antibodies for flow cytometry. The table lists all antibodies used in this study, including clone (when applicable), provider and catalogue number.

**A****IL-15 In Vivo Model****B****IL-2 or Poly I:C In Vivo Model**

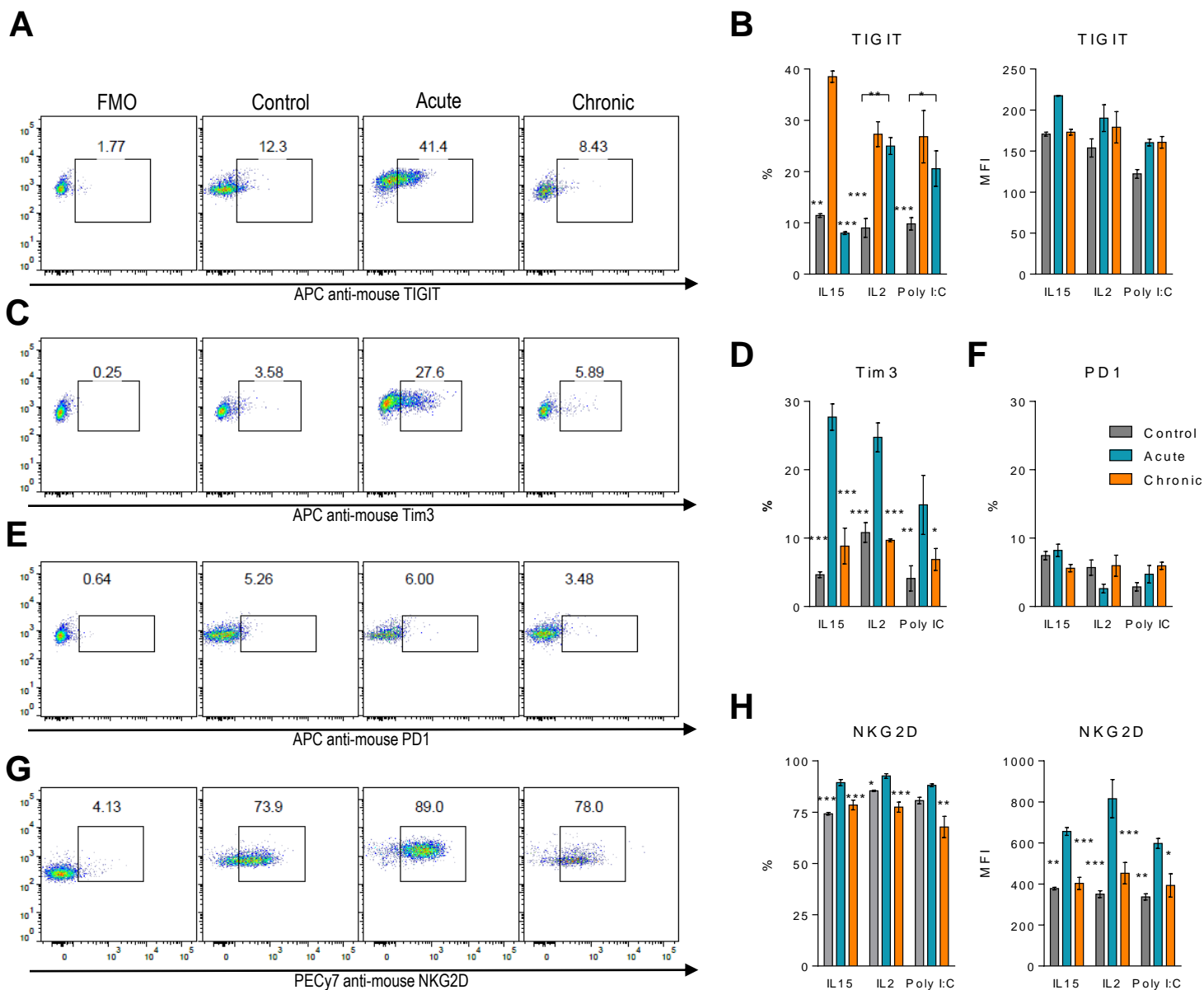
**Supplemental Figure 1. Schematic representation of the NK cell stimulation models.** In order to study the impact of in vivo sustained stimulation, mice received a variety of known NK cell activation reagents: IL-15/IL-15R $\alpha$  (2.5 $\mu$ g/3 $\mu$ g), IL-2 (5 $\times$ 10<sup>5</sup> IU) and the TLR3 ligand poly I:C (200 $\mu$ g). Chronic stimulation was achieved by continues i.p injections of the activation reagent at the indicated days for each model. Acute and resolved stimulation was induced by i.p injections of a given reagent during the early or late stage of the dosage regimen at the indicated days respectively. 200ul of Phosphate buffered saline (PBS) was given at the indicated times as control. **(A-B)** Dose regimen representation for the IL-15 (A) and the IL-2 and Poly I:C (B) stimulation models.



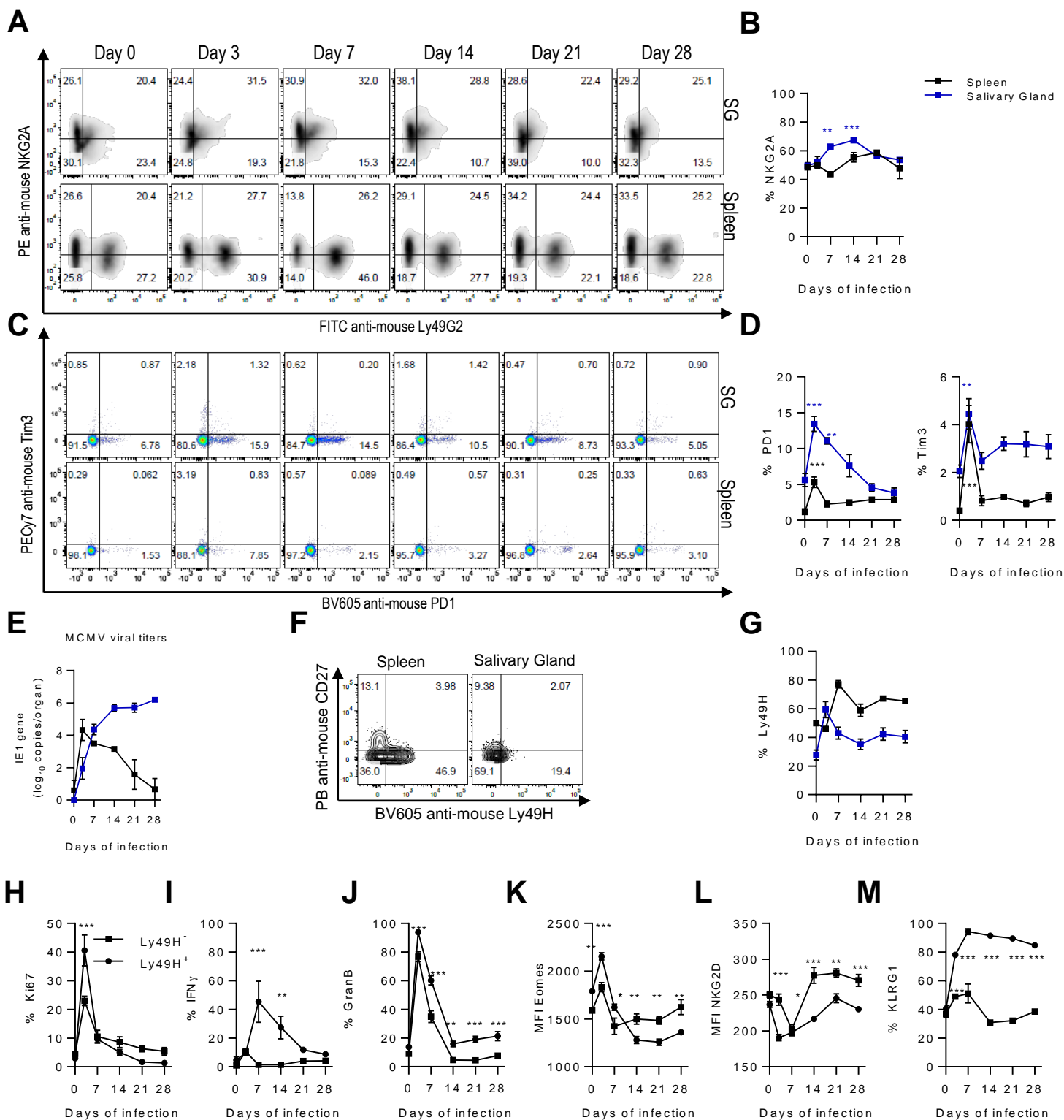
**Supplemental Figure 2. Exhaustion arises after prolonged IL-2 and Poly I:C stimulation.** C57BL/6 mice were treated with acute or chronic IL-2 or Poly I:C. Splenocytes were collected 24h after last treatment and evaluated for NK cell phenotype and function. **(A)** Multivariate heatmap analysis for IL-2 and poly I:C models. **(B)** Percentage of IFN $\gamma$  after 4h NK.1.1 stimulation is shown for gated NK cells. **(C)** Percentage of tumor cell lysis is shown. **(D)** Levels of IFN $\gamma$ , TNF $\alpha$ , IL-12, GM-CSF, CCL2, CCL3, CXCL9, CXCL10 found in the serum of treated mice. Data are representative of at least three independent experiments with an n=3 (mean  $\pm$  SEM). One-way ANOVA or two-way ANOVA (C) was done to assess significance (\* $p$ <0.05, \*\* $p$ <0.01, \*\*\* $p$ <0.001). Statistics are represented against the Acute treated group. No significant difference are found between the other groups unless it is indicated.



**Supplemental Figure 3. Impact of chronic stimulation on NK cell homeostasis. (A)** Total number of NK cells gated as CD3-NK1.1<sup>+</sup> is displayed for IL-15, IL-2 and Poly I:C stimulation models. **(B)** Representative dot-plots of immature-like (CD27<sup>-</sup>CD11b<sup>+</sup>) and mature-like (CD27<sup>+</sup>CD11b<sup>-</sup>) cells of gated CD3-NK1.1<sup>+</sup> NK cells is shown for spleen and BM in the IL-15 stimulation model. **(C)** Change of MFI for the IL2Rβ (CD122) expression after chronic stimulation on gated NK cells is shown. Data represents 3 independent experiments with 3 mice per group (mean ± SEM). Significant differences are displayed for comparisons with acutely stimulated groups (\*p<0.05, \*\*p<0.01, \*\*\*p<0.001). No significant differences were found between the other groups.

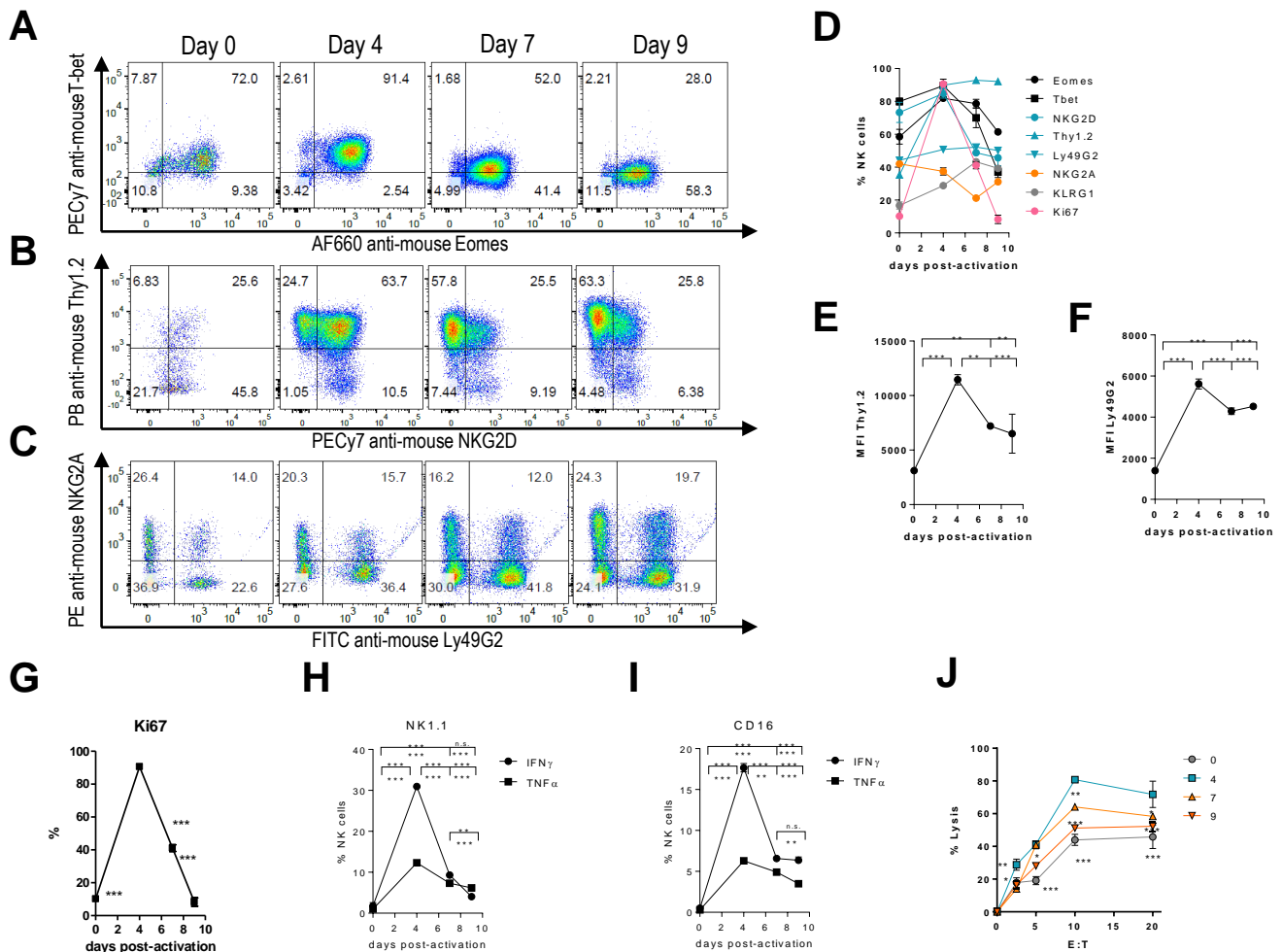


**Supplemental Figure 4. Impact of chronic stimulation on checkpoint inhibitors NK cell receptors. (A-B)** Representative dot plots (A), total percentage and MFI expression (B) of TIGIT on gated NK cells are shown. **(C-D)** Representative dot plots (C) and total percentage (D) of Tim3 on gated NK cells are shown. **(E-F)** Representative dot plots (E) and total percentage (F) of PD1 on gated NK cells are shown. **(G-H)** Representative dot plots (G), total Percentage and MFI expression (H) of NKG2D on gated NK cells are shown. Data represents at least 3 independent experiments with 3 mice per group (mean  $\pm$  SEM). Significant differences are displayed for comparisons with acutely stimulated groups (\* $p$ <0.05, \*\* $p$ <0.01, \*\*\* $p$ <0.001). No significant differences were found between the other groups.

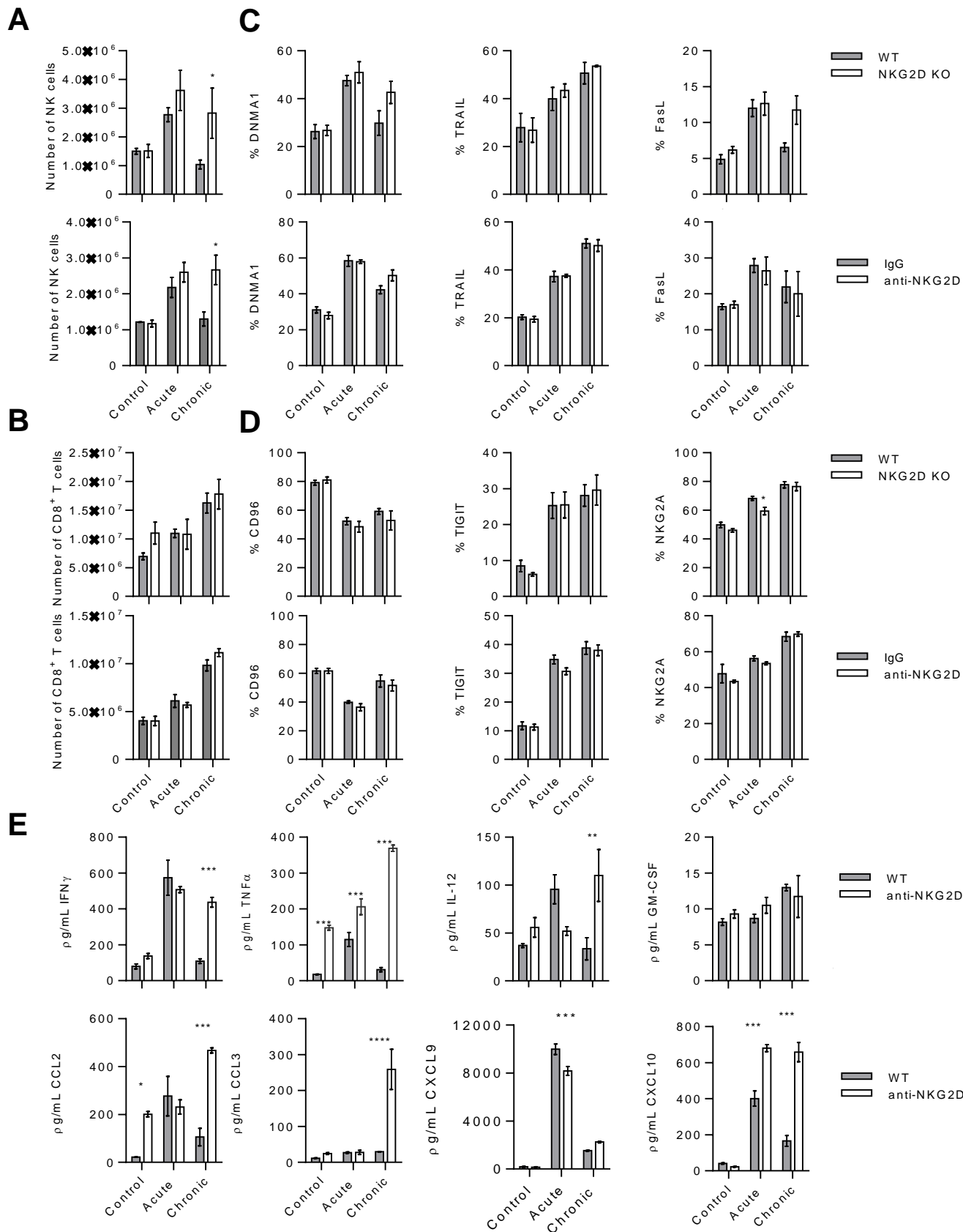


**Supplemental Figure 5. Expression of NK cell markers after chronic MCMV infection.** (A) Representative dot plots of the inhibitory receptors NKG2A and Ly49G2 is shown for gated NK cells derived from the spleen (black) or the salivary gland (blue) on MCMV infected mice. (B) Total percentage of NKG2A expression on gated NK cells is shown. (C-D) Representative dot plots (C) and total percentage (D) of PD1 and Tim3 on gated NK cells are shown. (E) MCMV viral titers (IE1 gene copies) of spleen and salivary gland at different time points after MCMV infection. (F) Representative dot-plots of CD27 and Ly49H expression from the spleen and salivary gland on non-infected mice (G) Total percentage of activation marker Ly49H on gated NK cells at different time points of MCMV infection on NK cells (CD3<sup>+</sup>NK1.1<sup>+</sup>). (H-M) Total percentage or MFI of Ki67 (H), IFN $\gamma$  (I), Granzyme B (J), Eomes (K), NKG2D (L) and KLRG1 (M) on Ly49H<sup>-</sup> (square symbol) or Ly49H<sup>+</sup> (circle symbol) NK cells is shown from the spleen of infected MCMV mice. IFN $\gamma$  was measure after NK1.1 stimulation. Data represents three independent experiments with 4-5 mice per group except in panel E which was done one time (mean  $\pm$  SEM). Significant differences are displayed for comparisons with non-infected controls at day 0. One-way ANOVA was used to assess (\* $p$ <0.05, \*\* $p$ <0.01, \*\*\* $p$ <0.001).

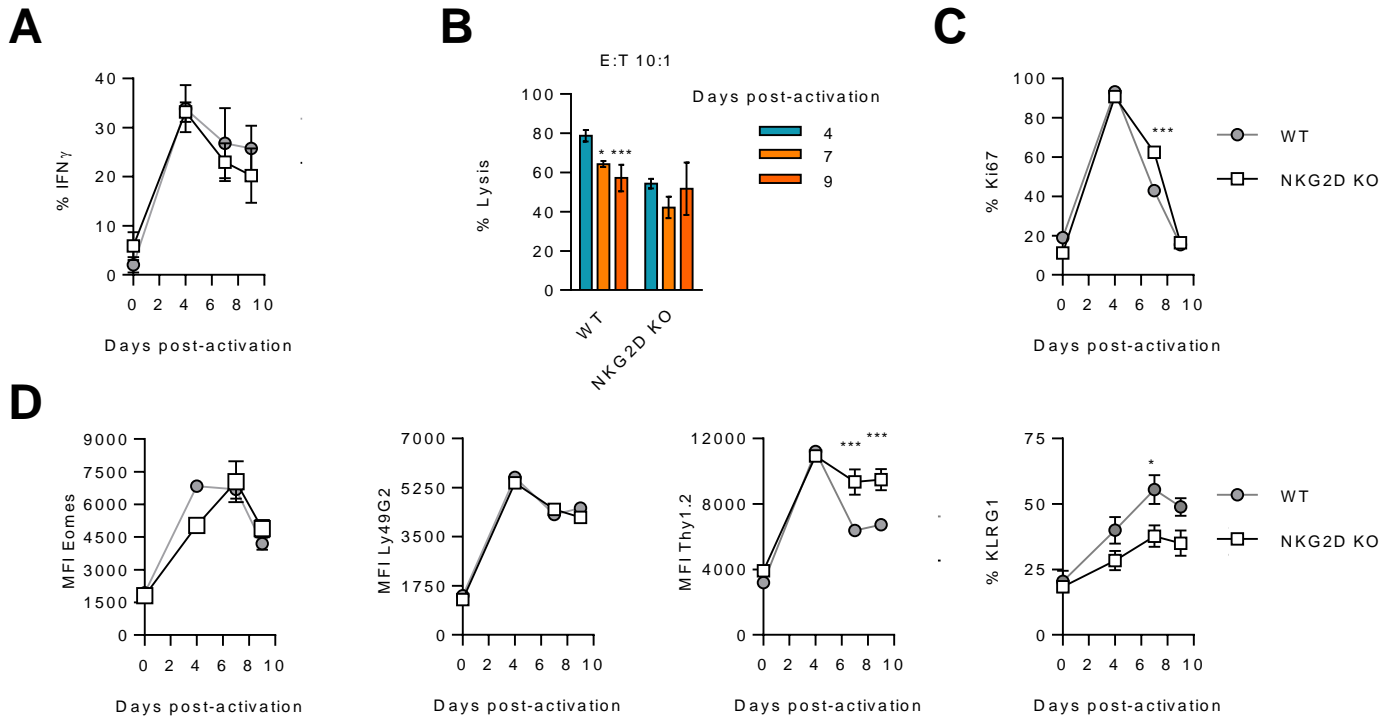




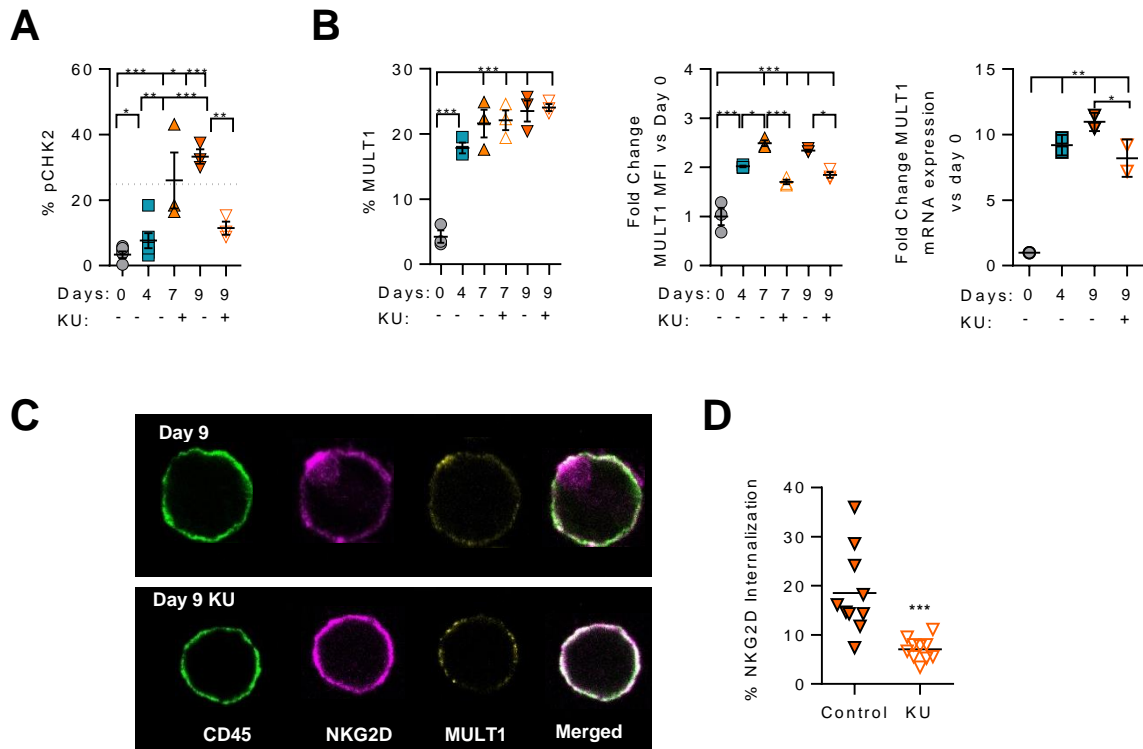
**Supplemental Figure 6. Long-term in vitro IL-2 stimulation recapitulates NCE phenotype.** Thy1.2<sup>-</sup> cells were cultured with IL-2 and adherent NK cells were collected and analyzed for NCE phenotype and function at different time points (control unstimulated: day 0; acutely stimulation: day 4; chronic stimulation: days 7 and 9). **(A)** Representative dot plots of Eomes and Tbet expression on gated NK cells (CD3<sup>+</sup>NK1.1<sup>+</sup>) is shown at different time points of stimulation. **(B)** Representative dot plots of NKG2D and Thy1.2 is shown for gated NK cells at different time points of stimulation. **(C)** Representative dot plots of the inhibitory receptors Ly49G2 and NKG2A is shown for gated NK cells at different time points of stimulation. **(D)** Total percentage of NK cell markers is shown at different time points of stimulation on gated NK cells. **(E-F)** MFI expression for Thy1.2 (E) and Ly49G2 (F) is shown for gated NK cells. **(G)** Percentage of cells expressing Ki67 on NK cells. **(H-I)** The percentage of IFN $\gamma$  and TNF $\alpha$  producing NK cells after NK1.1 (H) or CD16 stimulation (I). **(J)** Total percentage of tumor lysis is shown at different time points of activation. Data are representative of at least three independent experiments done by triplicate (mean  $\pm$  SEM). One-way ANOVA (D-I) or Two-way ANOVA (J) was done to assess significance (\* $p$ <0.05, \*\* $p$ <0.01, \*\*\* $p$ <0.001), which comparison was made against the peak of activation on day 4 (acute stimulation). No differences between the other groups were found unless otherwise indicated.



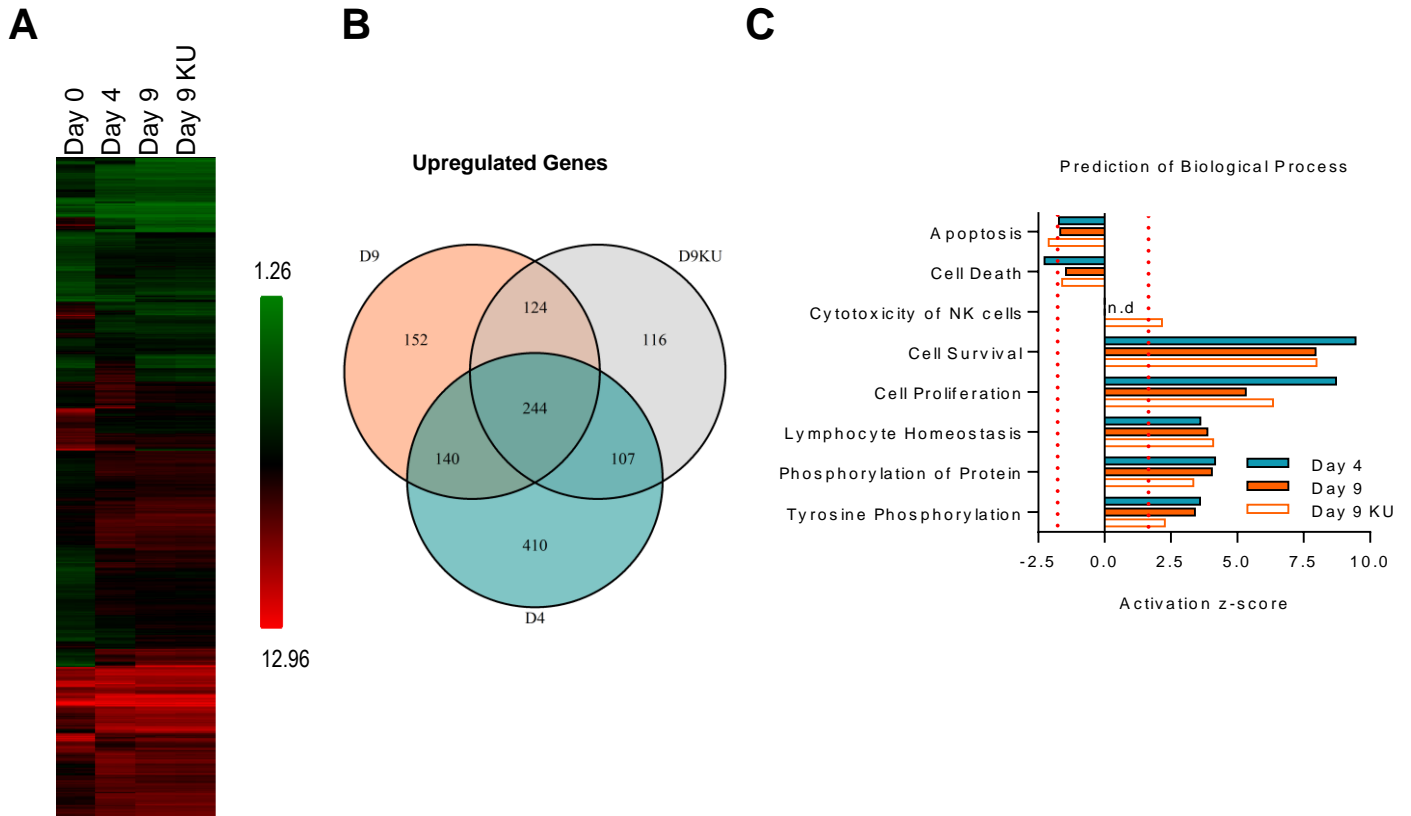
**Supplemental Figure 7. Impact of NKG2D deficiency on NK cells.** (A) Total number of NK cells is shown for in vivo IL-2 stimulated mouse where NKG2D was absence (upper level) or blockade (lower level) at the time of stimulation. (B) Percentage of NK cell activating receptors DNMA1, TRAIL and FasL gated on NK cells is shown for IL-2 treated WT and NKG2D KO mice (upper level) or control or anti-NKG2D mice (lower level). (C) Total number of CD3<sup>+</sup>CD8<sup>+</sup> T cells is shown L-2 treated WT and NKG2D KO mice (upper level) or control or anti-NKG2D mice (lower level). (D) Percentage of NK cell inhibitory receptors CD96, TIGIT and NKG2A gated on NK cells is shown L-2 treated WT and NKG2D KO mice (upper level) or control or anti-NKG2D mice (lower level). (E) Levels of IFN $\gamma$ , TNF $\alpha$ , IL-12, GM-CSF, CCL2, CCL3, CXCL9, CXCL10 found in the serum of treated mice. Data represents at least 3 independent experiments (mean  $\pm$  SEM). Significant differences are displayed for comparisons with WT and NKG2D deficient/blockade groups (\* $p$ <0.05, \*\* $p$ <0.01, \*\*\* $p$ <0.001).



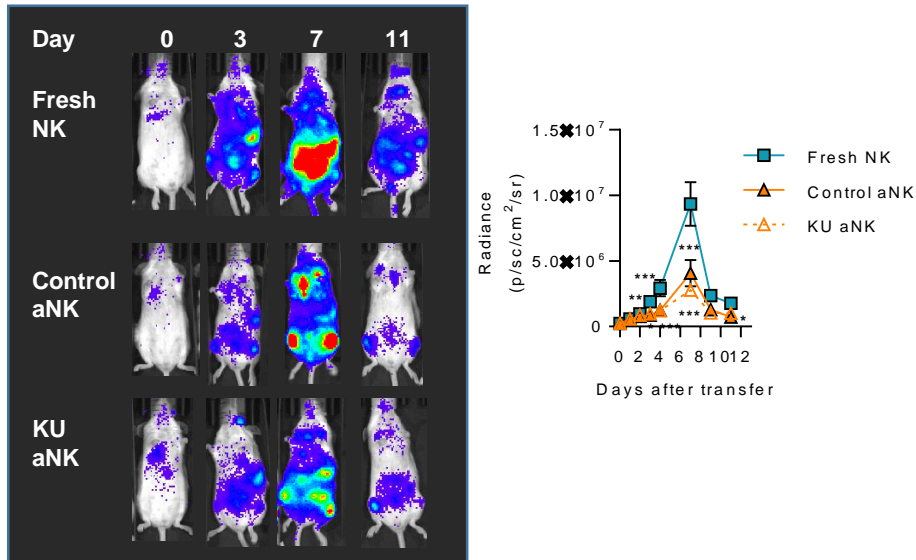
**Supplemental Figure 8. Long-term in vitro NK cell activation on NKG2D deficient mice has a reduced exhaustion phenotype.** (A) Percentage of IFN $\gamma$  production upon NK1.1 stimulation and tumor lysis at 10:1 E:T ratio for IL-2 activated WT and NKG2D KO NK cells. (B) Percentage of Ki67 on gated NK cells. (C) MFI or percentage of Eomes, Ly49G2, Thy1.2 and KLRG1 are shown for WT and NKG2D KO NK cells. Data are representative of three experiments performed in triplicate (mean  $\pm$  SEM). Two-Way ANOVA was used to assess significance. Significant differences are displayed for comparisons between WT and NKG2D KO at each time point (\* $p$ <0.05, \*\* $p$ <0.01, \*\*\* $p$ <0.001)



**Supplemental Figure 9. Impact of KU on NK cells during in vitro activation. (A)** The percentage of phosphorylation of the ATM-dependent protein Chk2 (pChk2) on gated NK cells. **(B)** Changes in the level of expression of MULT1 (percentage, MFI and mRNA) is shown for NK cells after KU treatment. **(C)** Representative immunofluorescence images of day 9 IL-2 in vitro stimulated NK cells after KU treatment showing CD45, NKG2D and MULT1 expression. **(D)** Total percentage of NKG2D internalization observed in immunofluorescence images in control or KU-treated NK cells collected on day 9. Data are representative of at least 3 independent experiments done in triplicate (mean  $\pm$  SEM). One-way ANOVA (A-B) or T-test study (B) were used to assess the significance between control and KU-treated NK cells (\* $p < 0.05$ , \*\* $p < 0.01$ , \*\*\* $p < 0.001$ ).



**Supplemental Figure 10. Molecular changes induced during long-term in vitro IL-2 activation.** **(A)** Heatmap representation of the gene expression profile of RNA obtained from freshly isolated NK cells (day 0) or NK cells collected at the peak of activation on day 4 or after exhaustion on day 9 during in vitro IL-2 stimulation with or without KU treatment (KU day 9). **(B)** Microarray analysis showing the overlap of up-regulated genes with significant differential expression on aNK cells at different time points when compared to gene expression of fresh NK cells (day 0). **(C)** Predicted biological processes affected by the up-regulated genes after IPA analysis is shown. Data are representative of 2 independent experiments done in duplicate (F-G). Dotted red lines indicate z-score value below 2.



**Supplemental Figure 11. In vivo proliferation and expansion of activated NK cells after adoptive transfer.** C57BL/6 L2G85 Luc<sup>+</sup> fresh NK cells or ex vivo IL-2 stimulated NK cells (control aNK or KU treated) were transferred into BALB/c Rag2<sup>-/-</sup>IL2R $\gamma$ <sup>-/-</sup> deficient mice and treated with 5 × 10<sup>4</sup> IU IL-2 for 7 days. NK cell proliferation, expansion and survival was measured by bioluminescence at different time points. **(A)** Representative images of bioluminescence signal at different time points for the different groups. **(B)** Graphical representation of the bioluminescence image. Data is representative of two independent experiments with 3 mice per group (mean ± SEM). One-way ANOVA was done to assess the significance (\*p < 0.05, \*\*p < 0.01, \*\*\*p < 0.001).